ЖЭТФ, 2012, том 142, вып. 4 (10), стр. 748–752

OPTIMIZATION OF THE MAGNETOCALORIC EFFECT IN Ni–Mn–In ALLOYS: A THEORETICAL STUDY

V. V. Sokolovskiy [a], ***V. D. Buchelnikov*** [a*], ***P. Entel*** [b]

[a] *Chelyabinsk State University, Department of Physics*
454001, Chelyabinsk, Russia

[b] *University of Duisburg-Essen, Faculty of Physics and CeNIDE*
47048, Duisburg, Germany

Received February 6, 2012

Based on *ab initio* and Monte Carlo simulations, we study the influence of the strength of the magnetic exchange parameters on the inverse and conventional magnetocaloric effect in the $Ni_{50}Mn_{34}In_{16}$ Heusler alloy using the mixed Potts and Blume–Emery–Griffiths model Hamiltonian. Within the proposed model, the temperature dependences of the magnetization, tetragonal deformation, and adiabatic temperature changes for magnetic field variation are obtained. It is first shown that a decrease in the magnetic exchange interactions leads to increased values of the magnetocaloric effect. We suppose that a reduction of the exchange interactions in the Ni–Mn–In alloy can be realized by the doping with nonmagnetic atoms such as B, Si, Zn, Cu, etc.

Magnetic cooling is attracting attention worldwide due to its potential use in solid state and environmentally friendly refrigeration technology, alternative to the conventional gas refrigeration technique [1]. Crucial for the success of magnetic cooling is the availability of materials showing a large magnetocaloric effect (MCE), which is related to the adiabatic temperature change ΔT_{ad} under application (removal) of a magnetic field. In materials undergoing a first-order magnetostructural transition or a second-order magnetic transition with a negative temperature coefficient of magnetization, the positive adiabatic temperature change is observed experimentally [1]. That MCE is usually called the direct or conventional MCE ($\Delta T_{ad} > 0$). In addition, in systems that undergo the first-order magnetostructural transition with a positive temperature coefficient of magnetization, the sign of ΔT_{ad} can be negative, in contrast to the positive sign in the conventional MCE [2–5]. Materials with such an inverse MCE find use as heat sinks for heat generated in refrigeration cycles involving conventional MCE materials [1–6].

The family of Ni–Mn–X (X = In, Sn, Sb) Heusler alloys has been identified to be a potentional source of both conventional and inverse MCEs [2–5]. Moreover, the Heusler alloys also show the ferromagnetic (FM) shape memory effect, large magnetoresistance, and magnetic superelasticity [5, 7–12]. The magnetization of these alloys drops abruptly following martensitic transformation from FM austenite to low-magnetic state martensite. The phase diagram of the $Ni_{50}Mn_{25+x}In_{25-x}$ system was recently investigated in detail in Refs. [7, 11, 12]. In this phase diagram, a narrow composition interval x = 8–10 is observed in which these alloys undergo a second-order magnetic phase transition to austenite and a first-order magnetostructural transformation from austenite to martensite under cooling. We note that both MCE types are observed in $Ni_{50}Mn_{25+x}In_{25-x}$ compounds with x ranging from 8 to 10. The sign of ΔT_{ad} can be negative at the first-order magnetostructural transition (T_m) and positive at the magnetic phase transition (T_C) [2–5]. Moreover, the absolute value of the inverse MCE ($\Delta T_{ad} < 0$) at the magnetostructural transition is larger than the corresponding value of the conventional MCE ($\Delta T_{ad} > 0$) at the Curie point. Therefore, the composition range of x between 8 and 10 in the $Ni_{50}Mn_{25+x}In_{25-x}$ system is particularly interesting because of the possibilities of a paramagnetic (PM) austenite transiting to an FM austenite and the FM austenite transforming to a low-magnetic martensite depending on the temperature and magnetic field. Such transitions could be of great technological importance in the magnetic cooling technology.

*E-mail: buche@csu.ru

Table 1. Magnetic exchange parameters (in meV) for $Ni_{50}Mn_{34}In_{16}$ obtained from *ab initio* calculations [16]

$Ni_{50}Mn_{34}In_{16}$	$J^m_{Mn_1-Mn_2}$	$J^m_{Mn_1-Ni}$	$J^m_{Mn_2-Ni}$
$c/a = 1$	-5.74	3.18	2.82
$c/a \neq 1$	-17.5	4.59	3.02

In a recent paper [13], we have performed Monte Carlo simulations of the conventional ($\Delta T_{ad} > 0$) and inverse ($\Delta T_{ad} < 0$) MCEs of the $Ni_{50}Mn_{34}In_{16}$ Heusler alloy, whereby the magnetic exchange parameters have been obtained from *ab initio* calculations using the spin polarized relativistic potential Korringa–Kohn–Rostoker code [14]. This code is based on the Green's functions and the theory in [15] for simulations of the exchange integrals between a pair of spins in the Heisenberg Hamiltonian. The chemical disorder was treated by the single-site coherent potential approximation. We present here some important results. The main magnetic exchange coupling constants of $Ni_{50}Mn_{34}In_{16}$ are listed in Table 1. The *ab initio* calculations have been done for the both cubic and tetragonal structures.

In Table 1, the Mn excess atoms located at the In sites are denoted as Mn_2, whereas Mn_1 are atoms occupying the regular Mn sublattice. We can see that the Mn_1–Ni (Mn_2–Ni) interactions are predominantly FM in the case of cubic and tetragonal states. Regarding the Mn_1–Mn_2 interaction, we can see that this interaction with the first coordination sphere in both austenitic and martensitic phases is antiferromagnetic (AFM). Moreover, it is strongest in the martensitic phase. The strong AFM interaction can explain the complex sequence of phase transitions that is observed experimentally for the Ni–Mn–In alloys. Moreover, the strong AFM interaction is also at the origin of the inverse MCE and exchange bias effect. When these *ab initio* coupling parameters are used in the effective spin model discussed in detail in [13, 16], which couples lattice and magnetic degrees of freedom, the results for the isothermal entropy change and adiabatic temperature change agree rather well with experiment.

In this paper, we investigate the influence of the strength of the magnetic exchange parameters on the inverse and conventional MCE by scaling all exchange parameters by the same factor. We show that different exchange interactions lead to various magnetocaloric values. This allows us to discuss in a simple manner what affects the magnitude of the MCE most and may therefore be taken as a guideline in extensive search for and synthesis of Heusler composites having the largest MCE. Our theoretical investigation is based on the microscopic mixed Potts and Blume–Emery–Griffiths model, which we have used in [13, 16].

We consider the magnetic and structural interactions on the realistic cubic and tetragonal lattice of Heusler alloys. For formation of the $Ni_{50}Mn_{34}In_{16}$ alloy, the excess of Mn_2 atoms is taken as corresponding to nominal compositions, whereas the configuration of the Mn_2 atoms in the In sublattice is set randomly. The magnetic subsystem is described by the mixed 3–5 Potts model, where 3 and 5 denote the respective numbers of spin states for the Ni and Mn atoms [13, 16]. Because the In atoms are nonmagnetic, we do not consider the Ni–In, Mn–In, and In–In interactions. In the structural subsystem, on the other hand, we consider interactions between all atoms. For the structural part, we have chosen the degenerate Blume–Emery–Griffiths model [13, 16], which allows describing the interaction between the elastic variables in the austenite and martensite.

Generalized Hamiltonian (1) consists of three parts: magnetic part (2), elastic part (3), and magnetoelastic interaction (4) [13, 16]:

$$H = H_m + H_{el} + H_{int}, \tag{1}$$

$$H_m = -\sum_{\langle i,j \rangle}^{NN} J^m_{i,j}\delta_{S_i,S_j} - g\mu_B H_{ext}\sum_i^N \delta_{S_i,S_g}, \tag{2}$$

$$H_{el} = -\left(J + K_1 g\mu_B H_{ext}\sum_i^N \delta_{\sigma_g\sigma_j}\right)\sum_{\langle i,j \rangle}^{NN}\sigma_i\sigma_j - K\sum_{\langle i,j \rangle}^{NN}(1-\sigma_i^2)(1-\sigma_j^2) - k_B T\ln(p)\sum_i(1-\sigma_i^2), \tag{3}$$

$$H_{int} = 2\sum_{\langle i,j \rangle}^{NN} U_{i,j}\delta_{S_i,S_j}\left(\frac{1}{2}-\sigma_i^2\right)\left(\frac{1}{2}-\sigma_j^2\right) - \frac{1}{2}\sum_{\langle i,j \rangle}^{NN} U_{i,j}\delta_{S_i,S_j}. \tag{4}$$

Here, $J^m_{i,j}$ is the exchange constant of the magnetic subsystem, $\langle i,j \rangle$ denotes the summation over the nearest neighbors, J and K are the exchange constants of the structural subsystem, $U_{i,j}$ and K_1 are the magnetoelastic interaction constants, T is the temperature, H_{ext} is the external magnetic field, and δ_{S_i,S_j} is the Kronecker

symbol, which restricts spin–spin interactions to the interactions between the same q_{Mn} states for Mn atoms and q_{Ni} states for Ni atoms, where q_{Ni} and q_{Mn} are the numbers of magnetic states of Ni and Mn atoms. For the Ni and Mn atoms, we respectively have three spin states $\{-1, 0, 1\}$ and five spin states $\{-2, -1, 0, 1, 2\}$ [13, 16]. Furthermore, S_i is a spin defined on the lattice site $i = 1, \ldots, N$; S_g is a ghost spin whose direction is determined by the external magnetic field, k_B is the Boltzmann constant, μ_B is Bohr's magneton, g is the Lande factor, p is the degeneracy factor that characterizes number of structural variants, $\sigma_i = 1, 0, -1$ represents the deformation state of each lattice site ($\sigma_i = 0$ corresponds to the undistorted state and $\sigma_i = \pm 1$ to distorted states), and σ_g is the ghost deformation state, whose value is that of a structural variant in the external magnetic field (positive H_{ext} favors deformation states coinciding with the ghost deformation state). Sums are taken over neighbor pairs in the first, second, and third Mn coordination spheres and in the first and second coordination spheres for the Ni atoms.

We note that in this paper, we only quote the Hamiltonian. The full information about each term of the Hamiltonian and basic equations for the calculation of the order parameters and MCE are presented in detail in Refs. [13, 16].

The magnetic and magnetocaloric properties for $Ni_{50}Mn_{34}In_{16}$ were simulated using the standard Metropolis algorithm [16]. Because we use a real lattice, the coordination number of nearest-neighbor atoms takes various values for each atom of the cubic and tetragonal unit cells. We therefore take neighboring pairs into account in the first, second, and third coordination spheres for Mn atoms and in the first and second coordination spheres for Ni atoms. In our simulations, we have used the lattice with 1098 Mn_1, 396 Mn_2, 1728 Ni, and 703 In atoms. For a given temperature, the number of the Monte Carlo steps on each site was taken $5 \cdot 10^5$. The simulation started from the FM martensitic phase. The system energy H and the order parameters m (magnetization) and ε (deformation) [16] were averaged over 1225 configurations for each of the 400 Monte Carlo steps. To obtain equilibrium values of H, m, and ε, the first 10^4 Monte Carlo steps were discarded. The degeneracy factor p and the Lande factor g were taken as $p = 2$ and $g = 2$. The value of dimensionless magnetoelastic interaction $K_1 = -1.5$ was chosen that the magnetic and structural transitions are coincident in an external magnetic field. The magnitudes of spin states (i. e., the q_{Ni} and q_{Mn} variables) were taken to correspond to a random number r such that $0 \le r \le 1$, and q_{Ni} and q_{Mn} were fixed according to the following scheme: if $0 \le r \le l/3$, then $q_{\mathrm{Ni}} = l$, $l = 1, 2, 3$, and if $0 \le r \le k/5$, then $q_{\mathrm{Mn}} = k$, $k = 1, \ldots, 5$.

Table 2. Scaling factors used in the model for $Ni_{50}Mn_{34}In_{16}$

Case	$c/a = 1$	$c/a \neq 1$
(a)	$n = 1$	$n = \{0.5, 0.75, 1.5, 2.0\}$
(b)	$n = \{0.5, 0.75, 1.5, 2.0\}$	$n = 1$
(c)	$n = \{0.5, 0.75, 1.5, 2.0\}$	$n = \{0.5, 0.75, 1.5, 2.0\}$

In the modeling of the inverse and conventional MCE, we have used the same structural and magnetoelastic model parameters as in [13]. We only changed the magnetic exchange constants of austenite and martensite listed in Table 1. The scaling factors n in Eq. (5), which define the new exchange parameters, are listed in Table 2 for the different cases considered here:

$$n = J^m_{i,j\_new} / J^m_{i,j\_old}, \tag{5}$$

where, J^m_{i,j_new} are the magnetic integrals used in this paper and J^m_{i,j_old} are the exchange constants from the *ab initio* calculations (see Table 1 and Ref. [13]).

Figure 1 presents the theoretical magnetization m and tetragonal distortion ε as functions of the temperature at different magnetic exchange constants for the $Ni_{50}Mn_{34}In_{16}$ alloy obtained for the different cases defined in Table 2. We note that we have presented the tetragonal distortion curve only for $n = 1$ because the behavior of the strain order parameter ε depends on the strength of the magnetic exchange parameters weakly. As can be seen from Fig. 1, the plots of m and ε coincide in the phase transition region at $T_m \approx 220$ K, which points to a coupled nature of the magnetostructural phase transition. We see from Fig. 1*a* that the decrease in exchange parameters in the martensite phase leads to a rapid drop of the magnetization curve at the magnetostructural phase transition, whereas the increasing exchange constants result in a less pronounced drop of the magnetization. We also note that the Curie temperature shifts slightly to the high-temperature region. In the second case, in Fig. 1*b*, increasing n leads to an increase in the Curie temperature, whereas the behavior of the magnetization curve at the magnetostructural transition differs slightly from the case $n = 1$. Conversely, if we decrease the exchange interactions in both martensite and austenite simultaneously (see Fig. 1*c*), we obtain a rapid drop of the magnetization at the

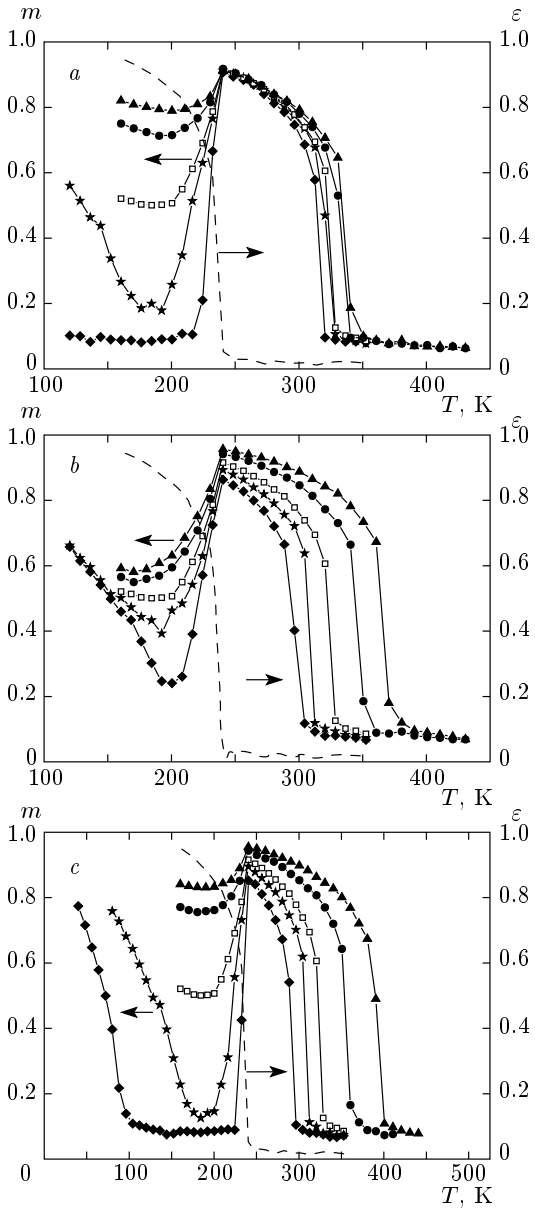

Fig. 1. Temperature dependence of the magnetization m and tetragonal distortion ε in $Ni_{50}Mn_{34}In_{16}$ alloy for different values of n in (5): $n = 0.5$ (♦), 0.75 (⋆), 1.0 (□), 1.5 (•), 2.0 (▲). The magnetic interactions are varied (a) only in martensite (see Table 2(a)); (b) only in austenite (see Table 2(b)); (c) in both martensite and austenite (see Table 2(c))

magnetostructural transition and lower Curie temperatures. The increase in the interaction strength results in a decrease in the magnetization drop at T_m and an increase in the Curie temperature T_C. We note that if we decrease the exchange interactions of martensite (see Fig. 1a,c), then the magnetic transition temperature from the AFM (or PM) state to mixed FM–AFM (or FM) martensite shifts to the low-temperature region.

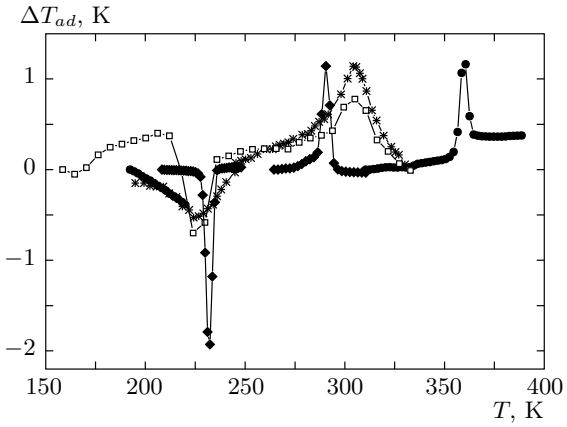

Fig. 2. Temperature dependence of the adiabatic temperature change in the $Ni_{50}Mn_{34}In_{16}$ alloy for different values of n in (5) in the magnetic field change $\Delta H_{ext} = 1$ T: $n = 0.5$ (♦), 1.0 (□), 1.5 (•). Lines with symbols (stars) are theoretical (experimental) curves of the MCE. Experimental data are taken from Ref. [4]

In Fig. 2, we show the temperature dependence of the adiabatic temperature changes in the $Ni_{50}Mn_{34}In_{16}$ alloy for different values of n and with the magnetic field varied from 0 to 1 T. The MCE curves are calculated using the scaling factors from Table 2(c). We can see from Fig. 2 that if the values of the exchange parameters are taken to be twice as small as the original *ab initio* exchange parameters ($n = 1.0$), then the value of the inverse MCE ($\Delta T_{ad} < 0$) increases by a factor of almost three, whereas the increase in exchange constants leads to a lower inverse MCE. Considering the conventional MCE ($\Delta T_{ad} > 0$), the change of the magnetic interaction strength affects the MCE value weakly.

In summary, we have investigated the influence of the strength of the magnetic exchange parameters on the inverse and conventional MCEs in the $Ni_{50}Mn_{34}In_{16}$ Heusler alloy by using *ab initio* and Monte Carlo calculations. Our simulations have shown that a decrease in the magnetic exchange interactions leads to increased values of the inverse MCE and to minor changes in the conventional MCE. We therefore suppose that a reduction of the exchange interactions (Mn_1–Mn_2, Mn_1–Ni, and Mn_2–Ni) in the Ni–Mn–In alloy can be realized by doping with nonmagnetic atoms such as B, Si, Zn, Cu, etc. In our opinion, the quartenary Ni–Mn–In–X Heusler alloys (X = B, Si, Zn, Cu, etc.) are good candidates for refrigerants of magnetic cooling technology.

This work was supported by the RFBR (grant No. 11-02-00601) and RF President grant No. MK-6278.2012.2.

REFERENCES

1. K. A. Gschneidner Jr., V. K. Pecharsky, and A. O. Tsokol, Rep. Prog. Phys. **68**, 1479 (2005).
2. T. Krenke, E. Duman, M. Acet et al., Nat. Mater. **4**, 450 (2005).
3. S. Aksoy, T. Krenke, M. Acet et al., Appl. Phys. Lett. **91**, 241916 (2007).
4. X. Moya, L. Manosa, A. Planes et al., Phys. Rev. B **75**, 184412 (2007).
5. A. Planes, L. Manosa, and M. Acet, J. Phys.: Condens. Matter **21**, 233201 (2009).
6. K. A. Gschneidner Jr. and V. K. Pecharsky, Int. J. Refrig. **31**, 945 (2008).
7. Y. Sutou, Y. Imano, N. Koeda et al., Appl. Phys. Lett. **85**, 4358 (2004).
8. A. N. Vasil'ev, V. D. Buchel'nikov, T. Takagi et al., Uspekhi Fiz. Nauk **173**, 577 (2003).
9. V. K. Sharma, M. K. Chattopadhyay, K. H. B. Shaeb et al., Appl. Phys. Lett. **89**, 222509 (2006).
10. B. Zhang, X. X. Zhang, S. Y. Yu et al., Appl. Phys. Lett. **91**, 012510 (2007).
11. X. Moya, L. Mañosa, A. Planes et al., Mater. Sci. Eng. A **438–440**, 911 (2006).
12. L. Manosa, X. Moya, A. Planes et al., Mater. Sci. Forum **583**, 111 (2008).
13. V. D. Buchelnikov, V. V. Sokolovskiy, S. V. Taskaev et al., J. Phys. D **44**, 064012 (2011).
14. H. Ebert, D. Kodderitzsch, and J. Minar, Rep. Prog. Phys. **74**, 096501 (2011).
15. I. Liechtenstein, M. I. Katsnelson, and V. A. Gubanov, J. Phys. F **14**, L125 (1984).
16. V. D. Buchelnikov, V. V. Sokolovskiy, H. C. Herper et al., Phys. Rev. B **81**, 094411 (2010).